Volume 11, Number 2, 2025

Modeling of Control Processes for Photovoltaic Power Plants

Oleh Maksymuk*

Lviv Polytechnic National University, 12 Stepana Bandery St., Lviv, 79013, Ukraine

Received: October 15, 2025. Revised: November 14, 2025. Accepted: December 16, 2025.

Abstract

The increase in electricity demand and the need for renewable energy are driving the rapid adoption of distributed generation sources, where photovoltaic (PV) generation holds a leading position. While PV systems convert free sunlight into electrical energy, their sensitivity to weather variations and lack of inertia limit widespread application without auxiliary energy storage systems. The variable nature of output power caused by dynamic solar radiation intensity changes is one of the main challenges for PV. In weak electrical grids, PV output power changes could significantly affect voltage levels, leading to electromagnetic compatibility issues and compromising the stability of generation sources and consumers. This paper focuses on studying short-time intensive solar irradiance changes the impact on a PV-rich medium voltage grid. Using the MATLAB/Simulink environment the rapid solar irradiance changes have been modeled to examine output PV power changes and the resulting voltage changes in the point of common coupling, depending on the control mode applied by the PV inverter.

Keywords: solar power plant; photovoltaic panel; reactive power; voltage change; electrical grid.

1. Introduction

While integrating new solar power plants into the existing grids, severe problems could arise due to photovoltaic (PV) output power changes. The dense cloud cover movement is one of the key weather factors. A sudden decrease in solar irradiation on the panels leads to a sharp drop in the PV output power and a voltage reduction at the point of common coupling (PCC). Conversely, overvoltage conditions appear under high power from PV and decreased PCC load. Such voltage changes could negatively impact consumers, particularly constant power load consumers, who restore their previous consumption level by increasing the current. This is especially dangerous for consumers, such as induction motors, as a voltage reduction leads to a decreased electromagnetic torque, potentially causing their disconnection from the grid, increased reactive power consumption, and the risk of voltage collapse.

2. Analysis of publications and research

Early studies on the integration of PV into the power grids [1]–[4] examine the dynamic response of photovoltaic generation systems to rapid changes in solar irradiance under high solar penetration conditions. The authors found that the voltage levels at the PCCs experience significant deviations during the sharp irradiance change periods if PV inverters are not equipped with reactive power control features. These studies also established that with an increasing level of PV penetration, the amplitude of such voltage changes grows substantially. The simulated impact of rapid solar radiation changes on the distribution grid shows that PV power variations pose a potential threat to voltage stability due to the rapid decrease in generated power, delays in transformer on-load tap changer (OLTC) operation, and dynamic

* Corresponding author. Email address: oleh.i.maksymuk@lpnu.ua

This paper should be cited as: O. Maksymuk. (2025). Modeling of control processes for photovoltaic power plants. *Energy Engineering and Control Systems*, Vol. 11, No. 2, pp. 99 – 108. https://doi.org/10.23939/jeecs2025.02.099

loads – particularly induction motors – which significantly affect operational stability. The authors emphasize that equipping inverters with reactive power control features brings a positive impact on power quality and voltage stability.

Recent studies focus on inverter control systems improvements for PV power plants [5], [6], particularly the application of smart inverters with extended reactive power control capabilities during the nighttime [7] and the implementation of grid-support functions during voltage sags and LVRT [8]. Some studies analyze dynamic stability and short-term voltage changes caused by cloud transients, load fluctuations, and fault conditions at the PCC [9], [10]. Other studies are devoted to the long-term PV operational stability research [11], [12], where the authors demonstrate that existing PV control techniques have several drawbacks in long-term voltage control efficiency and propose improved systems to address these issues.

3. Goal of the paper

The purpose of this research is to model the impact of the rapid solar irradiance changes on grid voltages under the different inverter control modes applied to the PV power plant; to analyze voltage changes caused by changes in the active power of PV; and to create a parameterized computer model for further research.

4. Initial data

The studied medium voltage (MV) power system diagram with a PV plant, which consists of panels themselves and inverters, and is connected to the external power grid via a 25 km 35 kV overhead transmission line, is shown in Fig. 1. All components of the power plant are connected to the 10 kV buses of a transformer with a rated power of 10 MVA. Local consumers are also connected to the 10 kV buses of the transformer. These buses are the point of common coupling (PCC) for all elements of the system.

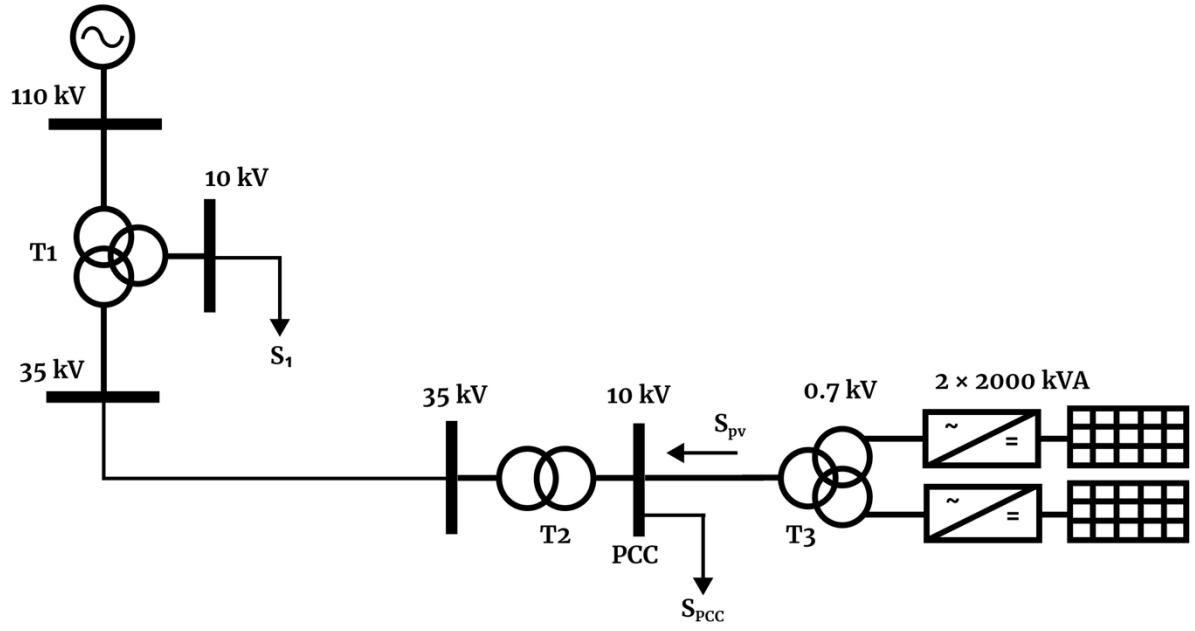

Fig. 1. Schematic diagram of the studied power system.

5. Modeling the inverter control processes

The MATLAB/Simulink environment was used for modeling. To model the power transformers' operation, catalog data and the "Three-Phase Transformer (Two Windings)" and "Three-Phase Transformer (Three Windings)" blocks were used; the parameters for the power transformers are provided in Table 1. The electrical connection between the Point of Common Coupling (PCC) transformer and the main system is established by an overhead power transmission line. The transmission line was modeled based on the catalog data for the AS-70/11 conductor and implemented using the "Three-Phase Series RLC Branch" block; the parameters for the transmission line are presented

in Table 2. To create the load at the PCC and at the beginning of the line, the "Three-Phase Series RLC Load" block was used; the parameters for the load are given in Table 3.

Table 1. Power transformer parameters.

Name of parameter	T1	T2	T3
Apparent power S, MVA	25	10	5
Winding 1 voltage V1, kV	115	38.5	10
Winding 2 voltage V2, kV	38.5	10.5	0.7
Winding 3 voltage V3, kV	11	–	0.7
Winding 1 R, p.u.	0.00375	0.00375	0.00465
Winding 2 R, p.u.	0.001343	0.00375	0.0093
Winding 3 R, p.u.	0.0081	–	0.0093
Winding 1 L, p.u.	0.04	0.04	0.0375
Winding 2 L, p.u.	0	0.04	0.075
Winding 3 L, p.u.	0.0675	–	0.075
Magnetization resistance, Rm, p.u.	806	690	544
Magnetization inductance, Lm, p.u.	145	127	114

Table 2. Power transmission lines parameters.

Name of parameter	Value
Length, km	25
R0, Ohms	0.306
X0, Ohms	0.444

Table 3. Load parameters.

Name of parameter	Value
P_l, MW	5
Q_l, MVar	0.5
P_{pcc}, MW	9.5
Q_{pcc}, MVar	1

The “PV Array” block was used to model the set of photovoltaic panels, connected in series to achieve desired voltage and in parallel for desired current, allowing simulation of output power change by causing incoming solar irradiance and temperature changes. The key parameters of the PV array are shown in Table 4. The “Three-Level NPC Converter” was chosen to model DC to AC converter, the inverter parameters are shown in Table 5. The low pass filter parameters are presented in Table 6.

Table 4. PV panels parameters.

Name of parameter	Value
Module data	Solar GS-420KR3
Maximum power, W	420.0526
Open-circuit voltage V_{oc}, V	60.65
Short-circuit current I_{sc}, A	9.12
Voltage at maximum power point V_{mpp}, V	48.73
Current at maximum power point I_{mpp}, A	8.62
Temperature coefficient of V_{oc}, %/deg. C	-0.36
Temperature coefficient of I_{sc}, %/deg. C	0.05
Parallel / Sequential	2 × 31s150p

Table 5. Inverter parameters.

Name of parameter	Value
Model type	Average model U ref controller
Diode on-state resistance, Ohms	0.001
Diode snubber resistance, Ohms	1e6
Diode snubber capacitance, F	inf
Diode forward voltage, V	1e-3
DC side snubber resistance, Ohms	inf

Table 6. Low pass filter parameters.

Name of parameter	Value
L1, mH	150
L2, mH	150
C, µF	500

The inverter control system is implemented based on a phase-locked loop (PLL), achieving inverter voltage synchronization with the measured voltage signal at the point of common coupling (PCC). While the inverter mimics the voltage, the operating modes are controlled by current. To simplify the inverter control system tuning, synchronization with an ideal voltage source has been used, which eliminates undesirable distortions of control signals caused by grid synchronization deviations. The PV system functional diagram is shown in Fig. 2.

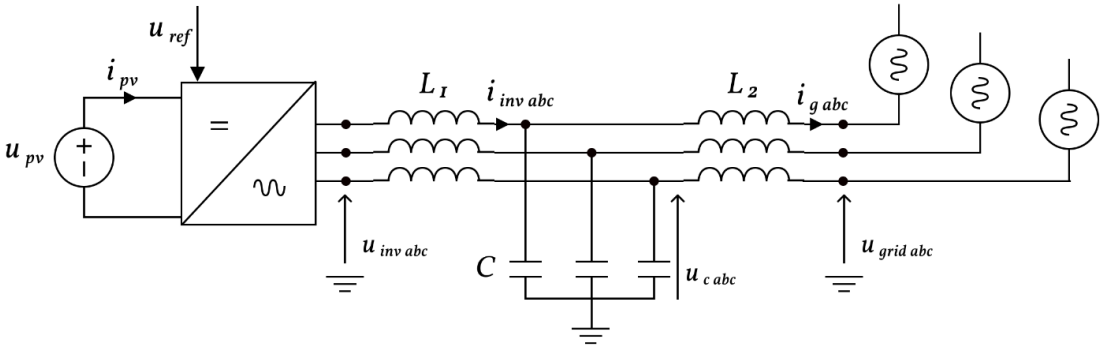

Fig. 2. Functional diagram of the PV system.

The control system was modeled based on Kirchhoff's voltage law for the inverter – filter inductance – filter capacitor loop in the complex-vector form of current and voltage values in the *dq0* coordinate system:

$$\overrightarrow{U_{inv}} = \overrightarrow{U_c} + j\omega L_1 \overrightarrow{I_{inv}}, \tag{1}$$

where $\overrightarrow{U_{inv}}$ is an inverter output voltage vector; $\overrightarrow{U_c}$ is a capacitor voltage vector; $\overrightarrow{I_{inv}}$ is a vector of current from inverter toward filter; L_1 is a filter inductance.

By decomposing the vectors (1) into their real and imaginary parts for each vector, the following expression is obtained:

$$U_{inv\,d} + jU_{inv\,q} = \left(U_{c\,d} + jU_{c\,q}\right) + j\omega L_1\left(I_{inv\,d} + jI_{inv\,q}\right), \tag{2}$$

where $U_{inv\,d}$ is a d-axis component of the inverter voltage; $U_{inv\,q}$ is a q-axis component of the inverter voltage; $U_{c\,d}$ is a d-axis component of the filter capacitor voltage; $U_{c\,q}$ is a q-axis component of the filter capacitor voltage; $I_{inv\,d}$ is a d-axis component of the inverter current; $I_{inv\,q}$ is a q-axis component of the inverter current.

For convenient application in the control system, they have been converted into a system of equations grouped by the values in the real plane and the imaginary plane:

$$\begin{cases} U_{ref\,d} = U_{c\,d} - \omega L_1 I_{inv\,q}; \\ jU_{ref\,q} = jU_{c\,q} + j\omega L_1 I_{inv\,d}. \end{cases} \quad (3)$$

To introduce the reference current values $I_{inv\,d\,ref}$ and $I_{inv\ q\,ref}$ into the system of equations (3), proportional–integral (PI) controllers outputs ($u_{d\,PI}, u_{q\,PI}$) are used, representing the operation of PI controller for the corresponding currents. Thus, the inverter control system takes the form of two control loops – the d-axis current control loop and the q-axis current control loop:

$$\begin{cases} U_{inv\ d\,ref} = u_{d\,PI}\,(I_{inv\,d\,ref} - I_{inv\,d}) - \omega L_1 I_{inv\,q} + U_{c\,d}; \\ U_{inv\,q\,ref} = u_{q\,PI}\,(I_{inv\,q\,ref} - I_{inv\,q}) + \omega L_1 I_{inv\,d} + U_{c\,q}, \end{cases} \quad (4)$$

where $u_{d\,PI}$ is output signal of PI controller for d-axis current; $u_{q\,PI}$ is output signal of PI controller for q-axis current; $I_{inv\,d\,ref}$ is reference current in d-axis; $I_{inv\,q\,ref}$ is reference current in q-axis.

D-q axes currents PI controllers' outputs:

$$u_{d\,PI}(t) = K_p\left(I_{inv\,d\,ref}(t) - I_{inv\,d}(t)\right) + K_i\int_0^t \left(I_{inv\,d\,ref}(\tau) - I_{inv\,d}(\tau)\right)d\tau; \quad (5)$$

$$u_{q\,PI}(t) = K_p\left(I_{inv\,q\,ref}(t) - I_{inv\,q}(t)\right) + K_i\int_0^t \left(I_{inv\,q\,ref}(\tau) - I_{inv\,q}(\tau)\right)d\tau, \quad (6)$$

where K_p is the proportional gain of the PI controller; K_i is the integral gain of the PI controller; τ is the integration variable.

Since $U_{inv\,d}$ and $U_{inv\,q}$ are large magnitude values, they must be normalized for use in the control systems:

$$\begin{cases} U_{pwm\ d\,ref} = U_{inv\ d\,ref}/(U_{dc}/2); \\ U_{pmw\ q\,ref} = U_{inv\,q\,ref}/(U_{dc}/2), \end{cases} \quad (7)$$

where $U_{pwm\ d\,ref}$, $U_{pmw\ q\,ref}$ are the reference voltage in d-q axes used for PWM generator control; U_{dc} is the DC bus voltage.

Since the variation of solar irradiance directly affects the generated active power, the reference current $I_{inv\,d\,ref}$ value must be carefully adjusted to obtain the maximum power from the solar panels on the one hand, and to maintain the system stability on the other. The d-axis current control equation takes the form of the PI controller output by continuously tracking the difference between the solar panel voltage and reference voltage:

$$I_{inv\,d\,ref} = u_{pv\,PI}\left(U_{pv\,ref} - U_{pv}\right), \quad (8)$$

where $U_{pv\,ref}$ is the reference voltage of the PV panels; U_{pv} is the measured voltage of the PV panels; $u_{pv\,PI}$ is the output signal of PI controller of PV voltage.

PV voltage PI controller output:

$$u_{pv\,PI}(t) = K_p\left(U_{pv\,ref}(t) - U_{pv}(t)\right) + K_i\int_0^t \left(U_{pv\,ref}(\tau) - U_{pv}(\tau)\right)d\tau, \quad (9)$$

where K_p is the proportional gain of the PI controller; K_i is the integral gain of the PI controller; τ is integration variable.

To model various techniques of reactive power control, the reference current value $I_{inv\,q\,ref}$ should be continuously adjusted by the control system as a function reacting to external parameters change depending on the specified reactive power control mode, $I_{inv\,q\,ref} = f(\varphi)$ for constant power factor or $I_{inv\,q\,ref} = f(U_{pcc})$ for Volt Var control.

To mimic the solar irradiance changes, the results of [13] were used. According to the source, the most probable ramp rate of solar irradiance during dense moving clouds lies in the range of $[-200 \ \ldots \ +200]$ $(W/m^2)/s$. The solar irradiance variations over 240 seconds used for further modeling are shown in Fig. 3.

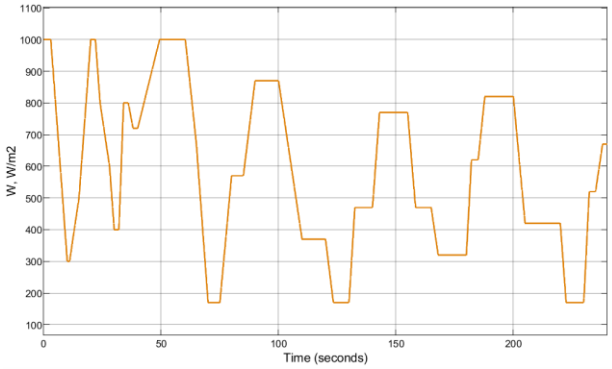

Fig. 3. Solar irradiance variation.

To configure the control system for constant power factor mode the PI controller has been used, which continuously adjusts the q-axis inverter current:

$$I_{inv\,q\,ref} = u_{\varphi\,PI}\left(P_{grid}\mathrm{tg}(\varphi_{ref}) - Q_{grid}\right), \tag{10}$$

where $\mathrm{tg}(\varphi_{ref})$ is a desired power factor for the control system to maintain; Q_{grid} is a measured value of inverter output reactive power injected into the grid; P_{grid} is a measured value of inverter output reactive power injected into the grid; $u_{\varphi\,PI}$ is the output signal of power factor PI controller.

Power factor PI controller output:

$$u_{\varphi\,PI}(t) = K_p\left(P_{grid}(t)\,\mathrm{tg}(\varphi_{ref}(t)) - Q_{grid}(t)\right) + K_i\int_0^t\left(P_{grid}(\tau)\,\mathrm{tg}(\varphi_{ref}(\tau)) - Q_{grid}(\tau)\right)d\tau\,, \tag{11}$$

where K_p is the proportional gain of the PI controller; K_i is the integral gain of the PI controller; τ is integration variable.

Depending on the selected reactive power control technique, a different voltage profile and amplitude of the voltage changes will be observed at the PCC. This is because modern PV inverters are capable not only of converting DC into AC, but also of operating as dynamically controlled devices, generating or consuming reactive power.

Fig.4 presents the simulation results to demonstrate the operating conditions of the PV inverter with a unity power factor. In this case, the inverter generates only active power, while its reactive power equals zero (Fig. 4,*a*). Fig. 4,*c* demonstrates the current component along the q-axis, which corresponds to reactive power, is adjusted by the control system (10) to maintain the inverter's output reactive power, whereas the d-axis component varies according to changes in solar irradiance (8). In this operating mode, the voltage at the PCC (Fig. 4,*b*) increases proportionally to the changes in active power generation. This phenomenon is explained by the fact that the power flow from the PV inverters to the grid reduces the voltage drop across the transmission line impedance, resulting in a voltage increase at PCC.

For comparison, Fig. 5 shows the system controls reactive power maintaining a fixed inductive power factor ($\cos\varphi_{inv} = 0.95$). In this case, in addition to active power generation coming from PV, the inverter consumes reactive power from the grid proportionally to the specified power factor. This is shown in Fig. 5,*c*, where the current component along the q-axis has a negative value. Fig. 5,*b* demonstrates voltage changes are significantly lower compared to the operating mode with $\cos\varphi_{inv} = 1$. This mode serves as an effective method for preventing overvoltage, particularly during periods of peak solar activity and low local demand.

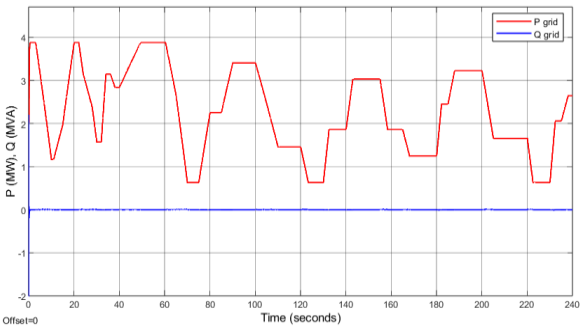

a – the output active and reactive powers of the PV power plant

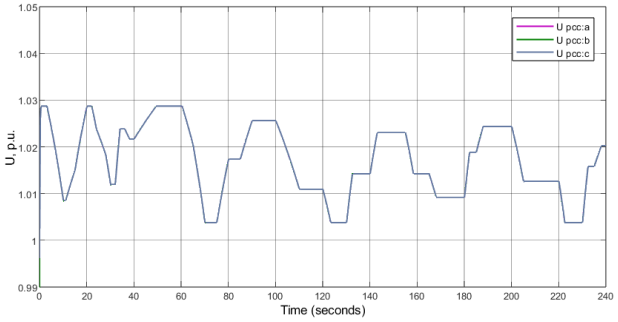

b – the voltage levels at the PCC

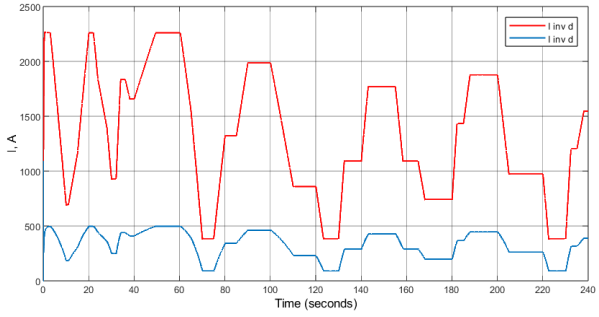

c – the inverter currents' magnitudes along the d and q axes

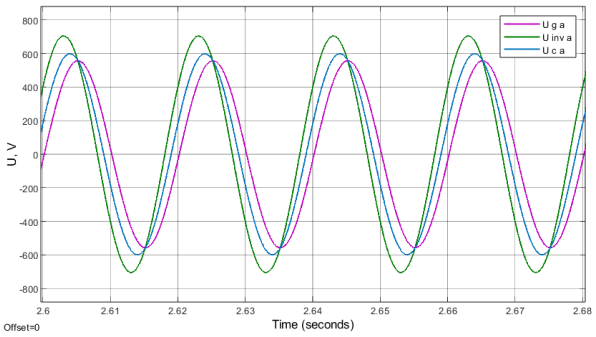

d – the waveforms of the inverter voltage, filter capacitor voltage, and grid voltage

Fig. 4. Simulation results of the constant power factor $\cos\varphi_{inv} = 1$ reactive power control mode.

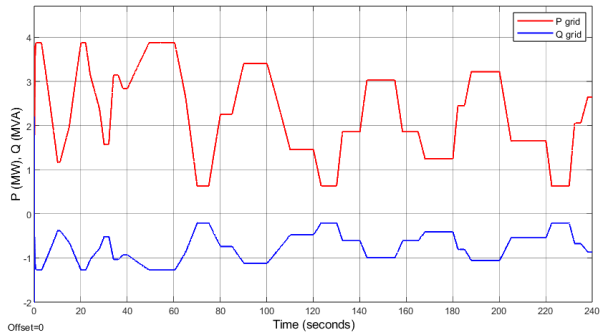

a – the output active and reactive powers of the PV power plant

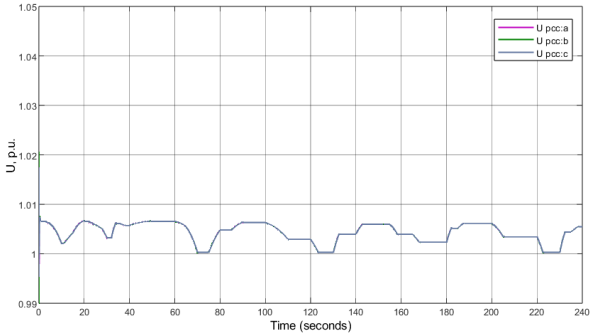

b – the voltage levels at the PCC

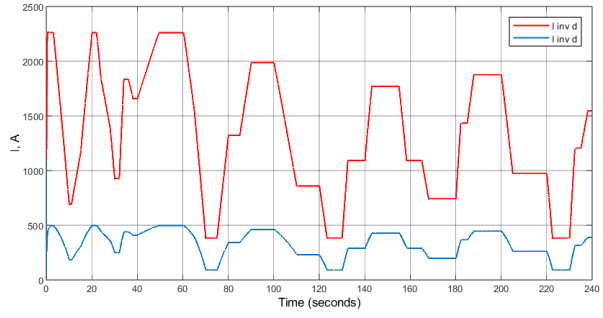

c – the inverter currents' magnitudes along the d and q axes

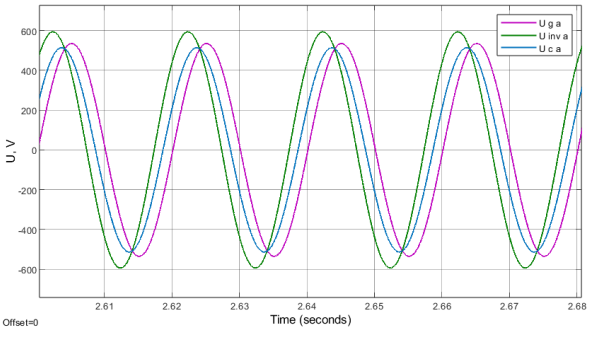

d – the waveforms of the inverter voltage, filter capacitor voltage, and grid voltage

Fig. 5. Simulation results of the constant power factor $\cos\varphi_{inv} = 0.95$ (inductive) reactive power control mode.

Fig. 6 displays the simulation results for the operating mode with a capacitive power factor, in which the inverter generates reactive power proportionally to the generated active power. In Fig. 6,*c*, the current along the q-axis has the

opposite direction and a greater amplitude compared to the inductive mode, which makes it an amplifier of voltage deviations during the active power generation changes caused by irradiance variations.

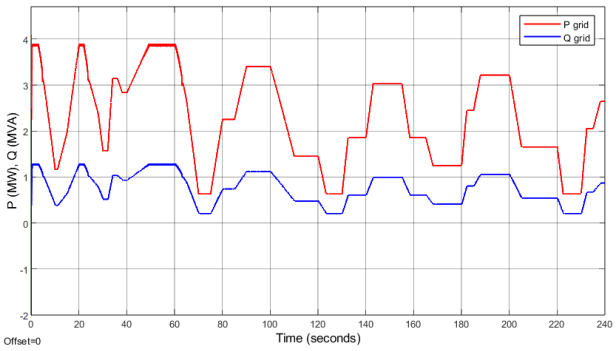

a – the output active and reactive powers of the PV power plant

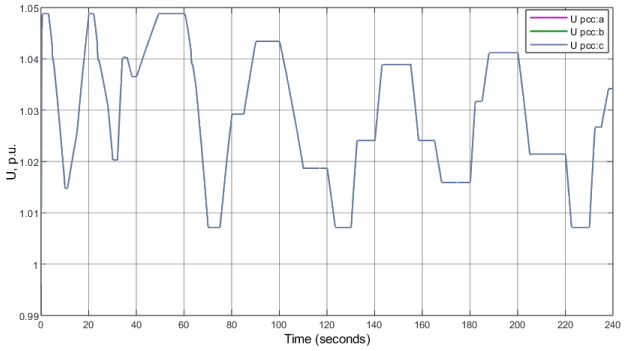

b – the voltage levels at the PCC

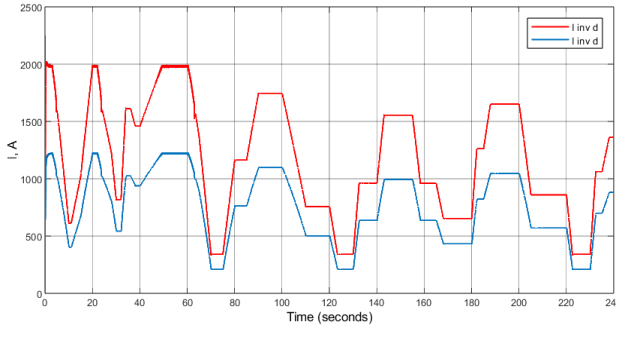

c – the inverter currents' magnitudes along the d and q axes

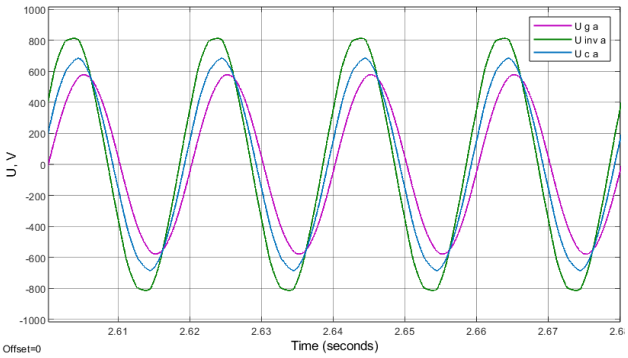

d – the waveforms of the inverter voltage, filter capacitor voltage, and grid voltage

Fig. 6. Simulation results of the constant power factor $\cos\varphi_{inv} = -0.95$ (capacitive) reactive power control mode.

By analyzing the plots presented in Fig. 4, Fig. 5 and Fig. 6, the common pattern of reactive power control in PV power plants with a constant reactive power factor has been identified and confirmed – a reduction of the amount of reactive power generated into the grid leads to a decrease of voltage changes in the PCC connection with electrical grid [14].

However, this control mode does not provide an adaptive response to variations in grid parameters and does not allow the inverters to maintain the voltage within a specified range, which restricts its application in the grids with a high share of distributed generation.

To implement the Volt Var reactive power control mode, a PI controller was used, whose output adjusts the inverter current magnitude along the q-axis based on measured and reference voltages at the PCC buses:

$$I_{inv\,q\,ref} = u_{vpcc\,PI}\left(U_{ref\,pcc} - U_{pcc}\right), \tag{12}$$

where $U_{ref\,pcc}$ is the reference value of the voltage to maintain at the PCC; U_{pcc} is the measured value of the voltage at the PCC; $u_{vpcc\,PI}$ is the voltage PI controller output.

Voltage PI controller output:

$$u_{vpcc\,PI}(t) = K_p\left(U_{ref\,pcc}(t) - U_{pcc}(t)\right) + K_i\int_0^t \left(U_{ref\,pcc}(\tau) - U_{pcc}(\tau)\right)d\tau\,, \tag{13}$$

where K_p is the proportional gain of the PI controller; K_i is the integral gain of the PI controller; τ is integration variable.

The simulation results of PV operating in the PCC voltage support mode is presented in Fig. 7. The variations of PV output power shown in Fig. 7,*a* indicate that the reactive power increases inversely proportionally to the changes in

active power, thereby compensating the variations in solar irradiance. While output power remains the same, Fig. 7,*b* demonstrates a stabilized voltage level at the PCC achieved solely through Volt Var reactive power control technique.

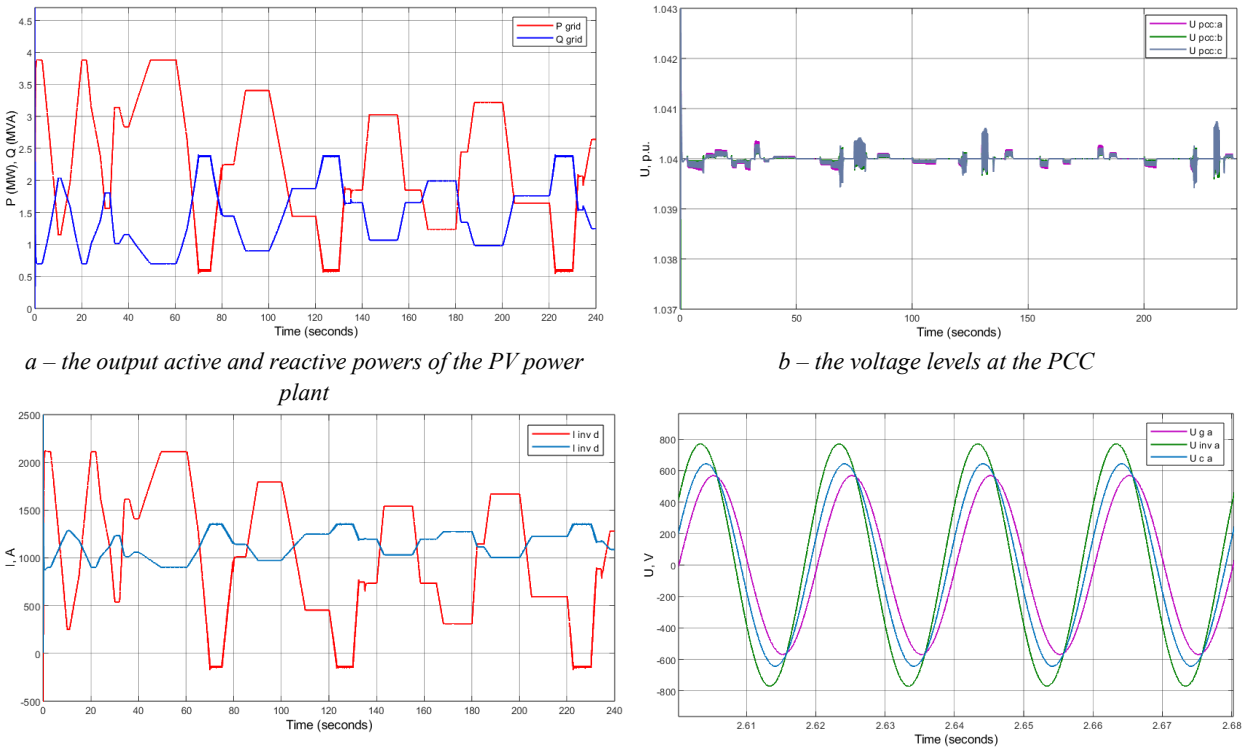

a – the output active and reactive powers of the PV power plant

b – the voltage levels at the PCC

c – the inverter currents' magnitudes along the d and q axes

d – the waveforms of the inverter voltage, filter capacitor voltage, and grid voltage

Fig. 7. Simulation results of the Volt Var voltage support reactive power control mode ($U_{pcc\,ref} = 1.04$).

6. Conclusion

In this study, a control system for a photovoltaic (PV) inverter was modeled, and a comparative analysis was conducted on reactive power control techniques for the PV plant integrated into a medium-voltage grid. The abrupt variations in solar irradiance, causing PV output power changes, were considered as a key factor in voltage changes. Results indicate that in grids featuring a substantial proportion of PV generation, power changes induced by the irradiance changes can cause significant voltage changes at the point of common coupling (PCC). The profiles of the voltage changes at PCC were examined depending on the reactive power control technique. The results show that inverters equipped with the reactive power control features are also effective support devices, maintaining voltage within predefined bounds.

Findings reveal that when incorporating PV power plants into suitably designed grids, voltage control can be performed without the use of expensive energy storage systems, utilizing only the reactive power capabilities of PV inverters. This underscores the role of PV power plants as a grid support asset, especially in scenarios with elevated renewable energy penetration.

References

[1] R. Yan, S. Roediger and T. K. Saha. (2011). Impact of photovoltaic power fluctuations by moving clouds on network voltage: A case study of an urban network. *AUPEC*, Brisbane, QLD, Australia, 2011, pp. 1-6.

[2] R. Yan and T. K. Saha. (2012). Investigation of Voltage Stability for Residential Customers Due to High Photovoltaic Penetrations. *IEEE Transactions on Power Systems*, vol. 27, no. 2, pp. 651-662, May 2012. https://doi.org/10.1109/TPWRS.2011.2180741.

[3] R. Yan and T. K. Saha. (2011). Investigation of voltage variations in unbalanced distribution systems due to high photovoltaic penetrations. *2011 IEEE Power and Energy Society General Meeting*. Detroit, MI, USA, pp. 1-8. https://doi.org/10.1109/PES.2011.6038977.

[4] F. C. L. Trindade, T. S. D. Ferreira, M. G. Lopes and W. Freitas. (2017). Mitigation of Fast Voltage Variations During Cloud Transients in Distribution Systems with PV Solar Farms. *IEEE Transactions on Power Delivery*, vol. 32, no. 2, pp. 921-932, April 2017. https://doi.org/10.1109/TPWRD.2016.2562922

[5] Three-Level Inverter Control Techniques: Design, Analysis, and Comparisons. (2021). *Elektronika Ir Elektrotechnika*, 27(3), 26-37. https://doi.org/10.5755/j02.eie.29015

[6] F. M. Aboshady, I. Pisica, A. F. Zobaa, G. A. Taylor, O. Ceylan and A. Ozdemir. (2023). Reactive Power Control of PV Inverters in Active Distribution Grids with High PV Penetration. *IEEE Access*, vol. 11, pp. 81477-81496, https://doi.org/10.1109/ACCESS.2023.3299351

[7] A. H. Javed, P. H. Nguyen, J. Morren and J. G. H. Slootweg. (2023). Using Smart PV Inverters for Reactive Power Management in Distribution Grids. *2023 IEEE Belgrade PowerTech*, Belgrade, Serbia, pp. 1-6. https://doi.org/10.1109/PowerTech55446.2023.10202681.

[8] Xu, Ke. (2024). Low-Voltage Ride-Through Technology in Photovoltaic Power Generation. Highlights in Science, Engineering and Technology. 81. 176-181. https://doi.org/10.54097/ypyswj45.

[9] A. Amanipoor, M. S. Golsorkhi, N. Bayati and M. Savaghebi. (2023). V-Iq Based Control Scheme for Mitigation of Transient Overvoltage in Distribution Feeders with High PV Penetration. *IEEE Transactions on Sustainable Energy*, vol. 14, no. 1, pp. 283-296, Jan. 2023. https://doi.org/10.1109/TSTE.2022.3211179

[10] K. Kawabe and K. Tanaka. (2015). Impact of Dynamic Behavior of Photovoltaic Power Generation Systems on Short-Term Voltage Stability. *IEEE Transactions on Power Systems*, vol. 30, no. 6, pp. 3416-3424, Nov. 2015, https://doi.org/10.1109/TPWRS.2015.2390649.

[11] Munkhchuluun, Enkhtsetseg & Meegahapola, L.G. & Vahidnia, Arash. (2020). Long-term voltage stability with large-scale solar-photovoltaic (PV) generation. *International Journal of Electrical Power & Energy Systems*. 117. 105663. https://doi.org/10.1016/j.ijepes.2019.105663.

[12] E. Munkhchuluun and L. Meegahapola. (2017). Impact of the solar photovoltaic (PV) generation on long-term voltage stability of a power network. *2017 IEEE Innovative Smart Grid Technologies - Asia (ISGT-Asia)*, Auckland, New Zealand, pp. 1-6, https://doi.org/10.1109/ISGT-Asia.2017.8378456

[13] A. R. Nikolopoulos, E. I. Batzelis, P. Lewin and N. Nikolaou. (2024). Statistical Analysis of Solar Irradiance Variability. *2024 IEEE Power & Energy Society General Meeting (PESGM)*, Seattle, WA, USA, 2024, pp. 1-5, doi: https://doi.org/10.1109/PESGM51994.2024.10689164.

[14] Yu. O. Varetskyy, V. M. Horban, Ya. S. Pazyna. (2016). Voltage variations in electrical microgrid with hybrid power plant. *Bulletin of Lviv Polytechnic National University: Electric Power and Electromechanical Systems*, No. 840, pp. 17-23. (in Ukrainian)

Моделювання процесів керування для фотоелектричних станцій

Олег Максимук

Національний університет «Львівська політехніка», вул. С. Бандери, 12, м. Львів, Україна

Анотація

Збільшення попиту на електроенергію та потреба в відновлюваній енергії сприяють швидкому впровадженню джерел розподіленого генерування, серед яких сонячна енергетика займає провідне місце. Фотоелектричні системи перетворюють енергію сонячного світла на електричну, проте чутливість до змін погодних умов обмежує їх широке застосування без допоміжних систем енергозбереження. Однією з головних проблем під час експлуатації фотоелектричних панелей є змінний характер вихідної потужності, спричинений змінами інтенсивності сонячної радіації. В слабких електричних мережах динамічні зміни активної потужності мають значний вплив на рівні напруги і, як наслідок, на електромагнітну сумісність і стійкість роботи джерел генерування та споживачів. На прикладі мережі з одностороннім живленням, використовуючи програмне середовище MATLAB/Simulink, досліджено вплив змін потужності фотоелектричної станції внаслідок динамічних змін сонячної радіації на рівні напруги в пункті спільного приєднання. Проаналізовано характер змін напруги залежно від способу керування інверторами фотоелектричних станцій.

Ключові слова: сонячна електростанція; фотоелектрична панель; реактивна потужність; зміна напруги; електрична мережа.